0026-895X/94/030532-08$03.00/0

MOLECULAR PHARMACOLOGY, 45:532-539

Two Distinct ATP Signaling Mechanisms in Differentiated Neuroblastoma × Glioma Hybrid NG108–15 Cells

SHEAU-HUEI CHUEH, LI-SUNG HSU, and SHU-LING SONG

Department of Biochemistry, National Defense Medical Center, Taipei, Taiwan, R.O.C. (S.-H.C., L.-S.H., S.-L.S.), and Institute of Biomedical Sciences, Academia Sinica, Taipei, Taiwan, R.O.C. (S.-H.C.)

Received June 30, 1993; Accepted November 23, 1993

SUMMARY

The ATP signaling mechanism in neuroblastoma × glioma hybrid NG108–15 cells differentiated by exposure to dibutyryl-cAMP was characterized. In cells loaded with fura-2, ATP rapidly raised the cytosolic Ca^{2+} concentration ($[Ca^{2+}]_i$); the magnitude of the rise was inversely proportional to the extracellular Na^+ concentration. Large increases in cytosolic Na^+ concentration, measured with the fluorescent Na^+ indicator sodium-binding benzofuran isophthalate, were dose-dependently elicited by ATP. ATP also evoked the entry of ethidium bromide into cells, and this process was inhibited by Mg^{2+}. Inositol-1,4,5-trisphosphate (IP_3) generation induced by ATP was totally blocked by removal of extracellular Ca^{2+}, but residual IP_3 generation still remained in nondifferentiated cells. In addition, ATP produced a concentration-, time-, and Mg^{2+}-dependent biphasic uptake of $^{45}Ca^{2+}$. A range of nucleotides and ATP analogues, including CTP, UTP, and GTP, induced only 9–29% of the ATP response. However, adenosine 5′-thiotriphosphate evoked 79% of ATP-induced $^{45}Ca^{2+}$ uptake. $^{45}Ca^{2+}$ uptake elicited by ATP could be potently blocked by purinoceptor antagonists, but other tested reagents less effectively blocked the action of ATP. When bradykinin was used as an agonist, the $[Ca^{2+}]_i$ rise was transient and was insensitive to the extracellular Na^+ concentration. Na^+ influx, entry of ethidium bromide, and $^{45}Ca^{2+}$ uptake were unaffected by bradykinin. Furthermore, bradykinin-evoked IP_3 generation was insensitive to extracellular Ca^{2+}. Neither ATP nor bradykinin had any effect on cAMP levels within cells. These data suggest that ATP induces a $[Ca^{2+}]_i$ rise in differentiated NG108–15 cells via two distinct Ca^{2+} influx mechanisms, i.e., a receptor-operated cation channel and pores formed by ATP^{4-}. These mechanisms are distinct from those elicited by bradykinin.

ATP serves as an extracellular transmitter molecule to evoke various cellular responses in many tissues (1). Evidence suggests that ATP exerts its action through specific receptors termed P_2 purinoceptors. On the basis of the potencies of the responses to various agonists, P_2 purinoceptors have been classified into five subclasses, namely P_{2x}, P_{2y}, P_{2z}, P_{2t}, and P_{2u} (2). Accordingly, six distinct intracellular signaling mechanisms are coupled to occupancy of P_2 purinoceptors in various tissues, (i) activation of phospholipase C, which in turn generates diacylglycerol and IP_3, subsequently triggering internal Ca^{2+} release (3); (ii) activation of a receptor-operated cation channel that is permeable to Ca^{2+} and Na^+ (4, 5); (iii) formation of pores by ATP^{4-}, allowing molecules to pass through after being screened nonspecifically by size (6, 7); (iv) activation or inhibition of adenylate cyclase, which consequently modulates cytosolic cAMP levels (8); (v) activation of phospholipase A_2 to release arachidonic acid, consequently followed by synthesis of its oxidative metabolites (9); and (vi) activation of phospholipase D (10). The first three mechanisms elicited by ATP result in an increase in $[Ca^{2+}]_i$. However, not all mechanisms are necessarily present within the same cell.

Previously, we reported that, in neuroblastoma × glioma hybrid NG108–15 cells differentiated by exposure to dibutyryl-cAMP, ATP specifically elevated $[Ca^{2+}]_i$. This process depended on the presence of extracellular Ca^{2+} (11). The ATP-induced $[Ca^{2+}]_i$ increase was not affected by pretreatment with either thapsigargin or bradykinin, indicating independence from the degree of filling of internal Ca^{2+} pools. We therefore suggested that the $[Ca^{2+}]_i$ rise induced by ATP is caused mainly by an influx of extracellular Ca^{2+}, which is distinct from the induction mechanism evoked by bradykinin. Briefly, bradykinin stimulates phospholipase C to generate IP_3 and diacylglycerol, and then IP_3 triggers Ca^{2+} release from internal Ca^{2+} stores (12, 13). The phospholipase C-independent increase in $[Ca^{2+}]_i$ in response to ATP that we observed in NG108–15 cells also occurs in a number of other cell types (14, 15).

NG108–15 cells have been used to study the signaling pathways for activation of various receptors. We have proposed two

This work was supported by a grant from the National Science Council, Republic of China (NSC81-0412-B016-542).

ABBREVIATIONS: IP_3, inositol-1,4,5-trisphosphate; SBFI, sodium-binding benzofuran isophthalate; AMPCPP, α,β-methylene-ATP; AMPPCP, β,γ-methylene-ATP; 2-MeS-ATP, 2-methylthio-ATP; ATPγS, adenosine 5′-thiotriphosphate; AMPPNP, 5′-adenylyl-β,γ-imidodiphosphate; PCMPS, *p*-chloromercuriphenylsulfonic acid; DIDS, 4,4′-diisothiocyano-2,2′-disulfonic acid stilbene; TMB-8, 8-(*N*,*N*-diethylamino)octyl-3,4,5-trimethoxybenzoate; IBMX, 3-isobutyl-1-methylxanthine; HEPES, 4-(2-hydroxyethyl)-1-piperazineethanesulfonic acid; $[Ca^{2+}]_i$, intracellular Ca^{2+} concentration.

distinct mechanisms for the $[Ca^{2+}]_i$ rise induced by ATP in NG108–15 cells, i.e., ion channels that are permeable to Ca^{2+} and Na^+ and pores formed by ATP^{4-} (11). Here we characterize further how the induction mechanism of ATP in dibutyryl-cAMP-differentiated NG108–15 cells differs from that in non-differentiated cells. The results confirm that bradykinin and ATP activate distinct signaling mechanisms. Direct evidence shows that ATP triggers Ca^{2+} influx through either ATP^{4-}-activated nonselective pores or ATP-operated cation channels. Furthermore, neither phospholipase C nor adenylate cyclase is activated by ATP in differentiated NG108–15 cells.

Materials and Methods

Culture of NG108–15 cells. NG108–15 cells obtained from Dr. M. Nirenberg, National Institutes of Health (Bethesda, MD), were used between passages 21 and 35. The cells were cultured in Dulbecco's modified Eagle's medium (with high glucose) supplemented with 10% fetal bovine serum, 100 μM hypoxanthine, 1 μM aminopterin, and 16 μM thymidine. Cells were grown at 37° in 100- × 20-mm tissue culture dishes (Falcon) in a humidified atmosphere of 10% CO_2/90% air. Differentiation was induced by incorporation of 1 mM dibutyryl-cAMP into the medium and reduction of serum to 5% for a period of 5 days. Half of the volume of growth medium was replaced daily with fresh medium.

Measurement of $[Ca^{2+}]_i$. NG108–15 cells (10^6 cells/ml) were loaded with fura-2 by incubation at 37° for 30 min with 5 μM fura-2/acetoxymethyl ester in buffer containing 150 mM NaCl, 5 mM KCl, 1 mM $MgCl_2$, 2.2 mM $CaCl_2$, 5 mM glucose, and 10 mM HEPES, pH 7.4 (designated as loading buffer). After loading, cells were washed twice, resuspended in loading buffer, and kept on ice before use. The fluorescence of cell suspensions (2×10^5 cells) was measured in a cuvette using a dual-excitation wavelength fluorometer (Spex; CM Systems). The $[Ca^{2+}]_i$ was calculated from the ratio between the fluorescence values at the two excitation wavelengths, as described previously (16). A K_d of 224 nM for fura-2 and Ca^{2+} equilibrium was used. For experiments in which Na^+ was omitted, the Na^+ in the loading buffer was replaced equiosmolarly by Tris. All experiments were performed at least three times using different batches of cells. Results from one representative experiment are illustrated graphically and mean ± standard deviation values for peak $[Ca^{2+}]_i$, calculated from n experiments, are shown.

Measurement of $^{45}Ca^{2+}$ uptake in NG108–15 cells. Aliquots of cell suspension (0.4 mg of cell protein) were added to test tubes containing 3 mM ATP, $^{45}Ca^{2+}$ (1 μCi/ml), and various agents (as indicated in the figures) in loading buffer, with a total assay volume of 220 μl. For experiments to measure the time dependence of Ca^{2+} uptake, we used single larger vials for uptake, with a starting volume of 2.6 ml, from which 0.2-ml samples were withdrawn at appropriate times; uptake was rapidly terminated as for individual tubes (see below). At indicated times, ATP-dependent Ca^{2+} uptake was terminated by addition of 4 ml of ice-cold loading buffer containing 1 mM $LaCl_3$, followed by immediate vacuum filtration of the cells onto Whatman GF/C glass fiber filters. After another four washes, radioactivity remaining on the filters was counted, and the amount of calcium that had accumulated within cells was thereby deduced.

Determination of intracellular Na^+ concentration. Cells (10^6 cells/ml) were loaded with the sodium indicator SBFI by incubation at 37° for 2 hr with 10 μM SBFI/acetoxymethyl ester and 0.024% (w/v) pluronic F-127 in loading buffer. After loading, cells were washed twice, resuspended in loading buffer, and kept on ice. The 340/380-nm fluorescence ratio of cell suspensions (4×10^5 cells), with an emission wavelength of 505 nm, was measured in a cuvette using a dual-excitation wavelength fluorometer (Spex; CM Systems). The increase in intracellular Na^+ concentration was expressed as the increase in the 340/380-nm fluorescence ratio, as described previously (17). All experiments were performed at least three times using different batches of cells. Results from one representative experiment are illustrated graphically and mean ± standard deviation values for the initial rate of change of the 340/380-nm fluorescence ratio, calculated from three experiments, are shown.

Determination of ethidium bromide uptake. Aliquots of cells (4×10^5 cells) were resuspended in 3 ml of loading buffer containing 25 μM ethidium bromide, in a cuvette. To calculate ethidium bromide uptake, fluorescence measurements were made using a Spex fluorometer (CM Systems), with 310- and 580-nm wavelengths for excitation and emission, respectively (18). All experiments were undertaken at least three times, with similar results. Results from one representative experiment are illustrated graphically.

Determination of IP_3 generation. IP_3 generation within cells activated by ATP or bradykinin was measured under the same conditions used for $[Ca^{2+}]_i$ measurement. Aliquots of cell suspensions (0.6 mg of cell protein) were incubated at room temperature for 15 sec with 3 mM ATP or 15 μM bradykinin, in a total volume of 100 μl of loading buffer, with or without Ca^{2+}. IP_3 generation was terminated by addition of 20 μl of 20% (v/v) perchloric acid and incubation at 4° for 20 min. The precipitated cells were removed by centrifugation at 12,000 × g for 5 min. The supernatant was neutralized to pH 7.5 with 1.5 N KOH and 60 mM HEPES, and precipitated $KClO_4$ was removed by centrifugation. Aliquots of supernatant were used for determination of IP_3. IP_3 was quantified by the D-*myo*-[^{3}H]IP_3 radioreceptor assay system (catalog no. TRK 1000; Amersham), as described in the manufacturer's instruction manual. In some experiments, nondifferentiated cells (without dibutyryl-cAMP treatment) were also used to determine the effect of extracellular Ca^{2+} on IP_3 production activated by ATP or bradykinin.

Measurement of cAMP production. Cells were first treated with 0.5 mM IBMX for 30 min in culture. After harvesting, aliquots of cells (0.6 mg of cell protein) were incubated at 37° for 15 min with 1 μM prostaglandin E_1, 10 μM leucine enkephalin, 15 μM bradykinin, or 3 mM ATP, in a total volume of 100 μl of loading buffer. cAMP production within cells was terminated by addition of 10 μl of 1 N HCl. Cells were then chilled on ice for 1 hr to extract cAMP. After boiling for 1 min, cells were centrifuged at 12,000 × g for 10 min and supernatants were neutralized to pH 7.4 with 1.5 N KOH and 60 mM HEPES. Aliquots of extracts were used for measurement of cAMP. cAMP concentrations were determined by the [^{3}H]cAMP assay system (catalog no. TRK 432; Amersham), as described in the manufacturer's instruction manual.

Materials and miscellaneous procedures. Dulbecco's modified Eagle's medium, fetal bovine serum, and hypoxanthine/aminopterin/thymidine were purchased from GIBCO. The fluorescent Ca^{2+} indicator fura-2/acetoxymethyl ester and the Na^+ indicator SBFI/acetoxymethyl ester were obtained from Molecular Probes (Eugene, OR). ATP, bradykinin, prostaglandin E_1, leucine enkephalin, IBMX, ADP, AMP, ruthenium red, DIDS, diltiazem, Basilen Blue E-3G, Cibacron Blue 3GA, ethidium bromide, and PCMPS were purchased from Sigma Chemical Co. (St. Louis, MO). 2-MeS-ATP, AMPCPP, ryanodine, and TMB-8 were obtained from Research Biochemicals Incorporated (Natick, MA). CTP, UTP, GTP, AMPPCP, ATPγS, and AMPPNP were supplied by Boehringer Mannheim (Mannheim, Germany). $^{45}Ca^{2+}$ (35.12 mCi/mg) was bought from New England Nuclear (Boston, MA). The [^{3}H]IP_3 assay system and [^{3}H]cAMP assay system were obtained from Amersham Corp. The chloride salts of Ni^{2+}, Ba^{2+}, Sr^{2+}, Co^{2+}, Mn^{2+}, Cd^{2+}, and La^{3+} metal ions were of the highest available grade from Merck (Darmstadt, Germany). All other chemicals used were of analytical grade and were obtained from Merck.

Protein concentrations were determined by the method of Lowry *et al.* (19), using standards of bovine serum albumin. All experiments for measurements of $^{45}Ca^{2+}$ uptake, cAMP production, and IP_3 generation were carried out at least three times in triplicate, with similar results, and the data presented are mean ± standard deviation values from one representative triplicate experiment.

Results

The effect of extracellular Na^+ concentration on the ATP- or bradykinin-induced $[Ca^{2+}]_i$ rise is shown in Fig. 1. The

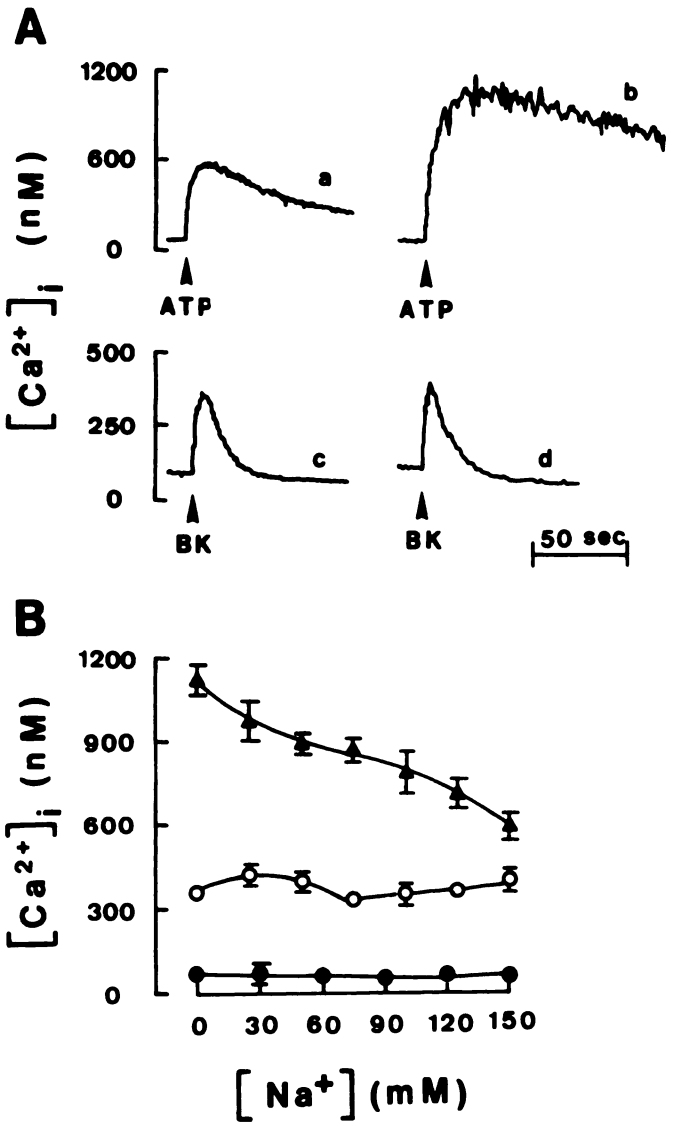

Fig. 1. Effect of extracellular Na^+ on $[Ca^{2+}]_i$ rise evoked by ATP or bradykinin (*BK*) in NG108–15 cells. A, ATP (3 mM) or bradykinin (15 μM) was added as indicated (*arrowheads*) to fura-2-loaded NG108–15 cells in the presence (*traces a* and *c*) or absence (*traces b* and *d*) of extracellular Na^+. In *traces b* and *d*, Na^+ was replaced by Tris equiosmolarly. B, The basal level (●) and the maximal levels of $[Ca^{2+}]_i$ evoked by bradykinin (○) or ATP (▲), measured at various concentrations of extracellular Na^+, are illustrated. Data shown are the mean ± standard deviation of three independent experiments.

extracellular Na^+ concentration was changed by replacing Na^+ in the loading buffer equiosmolarly with Tris. In response to 3 mM ATP, in the presence of 150 mM extracellular Na^+, the $[Ca^{2+}]_i$ of NG108–15 cells rapidly increased from a mean resting level of 70 ± 4 nM (mean ± standard deviation, $n = 12$) to a mean peak of 600 ± 40 nM ($n = 12$) (Fig. 1A, *trace a*). When extracellular Na^+ was completely replaced with Tris, the resting $[Ca^{2+}]_i$, 78 ± 2 nM ($n = 12$), showed a smaller rise. However, the peak $[Ca^{2+}]_i$ elicited by 3 mM ATP was greatly elevated to 1090 ± 60 nM ($n = 12$) (Fig. 1A, *trace b*). After reaching the peak, the $[Ca^{2+}]_i$ decreased to a mean plateau level of 198 ± 10 nM in the Na^+-containing solution and 768 ± 42 nM in the Na^+-free bathing solution, by 120 sec after ATP addition. Bradykinin (15 μM) caused a smaller rise in $[Ca^{2+}]_i$ than did ATP. The mean peak levels were 395 ± 25 nM ($n = 8$) and 387 ± 23 nM ($n = 8$) in the presence and absence of extracellular Na^+, respectively (Fig. 1A, *traces c* and *d*). Therefore, there was no clear distinction in the $[Ca^{2+}]_i$ rise stimulated by bradykinin between the Na^+-containing and Na^+-free solutions. In addition, the $[Ca^{2+}]_i$ rise activated by bradykinin declined to the basal level within 30 sec after bradykinin addition (Fig. 1A, *traces c* and *d*). Fig. 1B illustrates the dependence of the changes in $[Ca^{2+}]_i$ elicited by ATP or bradykinin on extracellular Na^+ concentration. There was a negative linear relationship between the concentration of Na^+ and rises in $[Ca^{2+}]_i$ induced by ATP. Thus, the magnitude of the $[Ca^{2+}]_i$ rise decreased as the extracellular Na^+ was increased. On the other hand, resting $[Ca^{2+}]_i$ or bradykinin-induced $[Ca^{2+}]_i$ changes remained at the same level without significant difference for all extracellular Na^+ concentrations tested (Fig. 1B).

The results described above suggest that ATP may activate a cationic channel that is nonselective for Na^+ and Ca^{2+}. We therefore examined the change in cytosolic Na^+ level elicited by ATP or bradykinin by using the 340/380-nm SBFI fluorescence ratio. SBFI has been proven to be a Na^+-responsive indicator (17). The 340/380-nm fluorescence ratio of SBFI correlates linearly with cytosolic Na^+ levels in the physiological concentration range (20). Fig. 2 depicts the response of the 340/380-nm fluorescence ratio within NG108–15 cells to stimulation by ATP or bradykinin. Upon addition of 3 mM ATP, the fluorescence ratio increased immediately and reached a plateau within 50 sec; thereafter, it remained steady over several minutes (Fig. 2A, *trace b*). Furthermore, the magnitude of the increase in the 340/380-nm fluorescence ratio depended on the ATP concentration (Fig. 2A). Fig. 2B summarizes the statistical data. The dependence of the initial rate of fluorescence change on the ATP dose (Fig. 2B) contrasts with the lack of change in fluorescence ratio observed when cells were treated with 15 μM bradykinin (Fig. 2A, *trace d*), a well characterized agonist that activates phospholipase C (12).

ATP^{4-} has been proposed to form pores in many cells (1, 6, 7) and might be responsible for the effect of ATP on $[Ca^{2+}]_i$ rise in NG108–15 cells (11, 21). We therefore examined the effect of ATP on ethidium bromide uptake, to assess membrane permeabilization. The fluorescence of ethidium bromide-DNA complexes within NG108–15 cells increased steadily upon ATP addition; half-maximal responses occurred after 60 sec (Fig. 3, *trace e*). To examine whether reduction of ATP^{4-} lowered the permeabilization of the membrane by resealing it, 1 mM Mg^{2+} was added at various times after ATP addition. The fluorescence increase could be halted by the addition of $MgCl_2$ at any time (Fig. 3, *traces b–d*). On the other hand, no fluorescence increase could be detected after addition of bradykinin to NG108–15 cells (Fig. 3, *trace a*).

Previously, using dibutyryl-cAMP-differentiated cells, we have shown that the $[Ca^{2+}]_i$ rise stimulated by ATP depends absolutely on extracellular Ca^{2+} (11). We therefore examined the effect of extracellular Ca^{2+} on ATP-induced IP_3 production. Table 1 illustrates agonist-stimulated IP_3 generation. Both differentiated and nondifferentiated cells were challenged with ATP or bradykinin in the presence or absence of extracellular Ca^{2+}. In the presence of Ca^{2+}, ATP and bradykinin elicited IP_3 generation of 48.1 ± 5.1 and 53.8 ± 3.2 pmol/mg, respectively, with a basal value of 11.1 ± 1.3 pmol/mg in differentiated cells. The removal of extracellular Ca^{2+} reduced the IP_3 generation by approximately 51%, 88%, and 54% in basal, ATP-stimulated, and bradykinin-stimulated cells, respectively. Thus, in the absence of extracellular Ca^{2+} the IP_3 generation evoked by

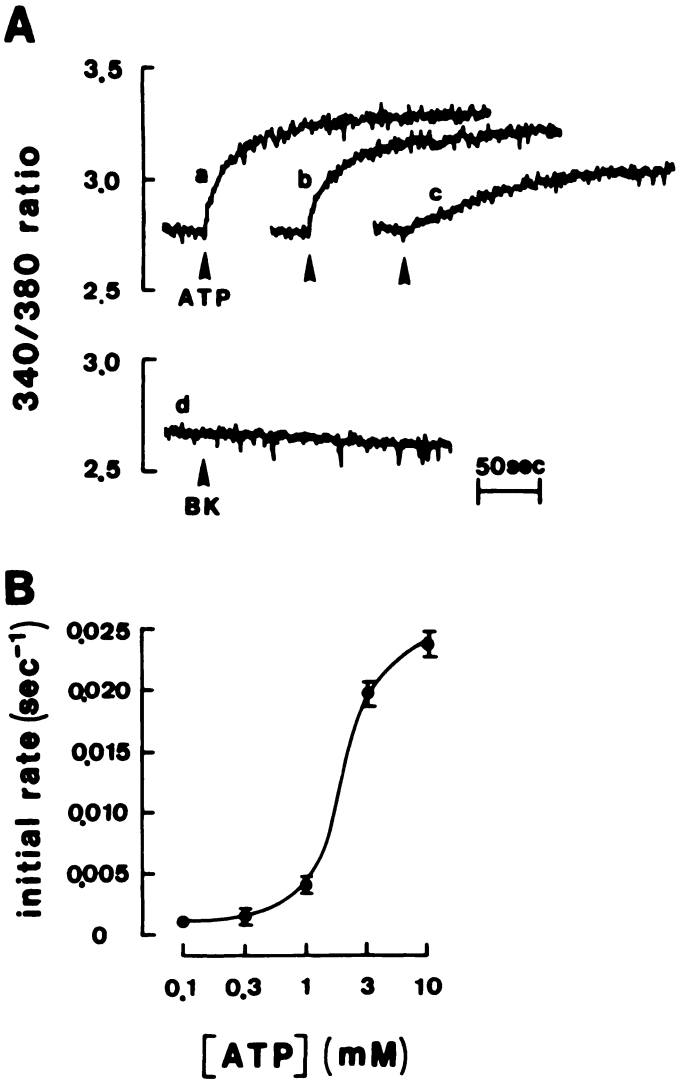

Fig. 2. Effect of extracellular ATP on intracellular Na^+ concentration in NG108–15 cells. A, ATP (*trace a*, 10 mM; *trace b*, 3 mM; *trace c*, 1 mM) or bradykinin (*BK*) (15 μM) (*trace d*) was added as indicated (*arrowheads*) to SBFI-loaded-NG108–15 cells. The SBFI fluorescence ratio (340/380 nm) was monitored. B, Various concentrations of ATP were added to cells and the initial rate of SBFI fluorescence ratio change is demonstrated. Data in B are the mean ± standard deviation from triplicate assays.

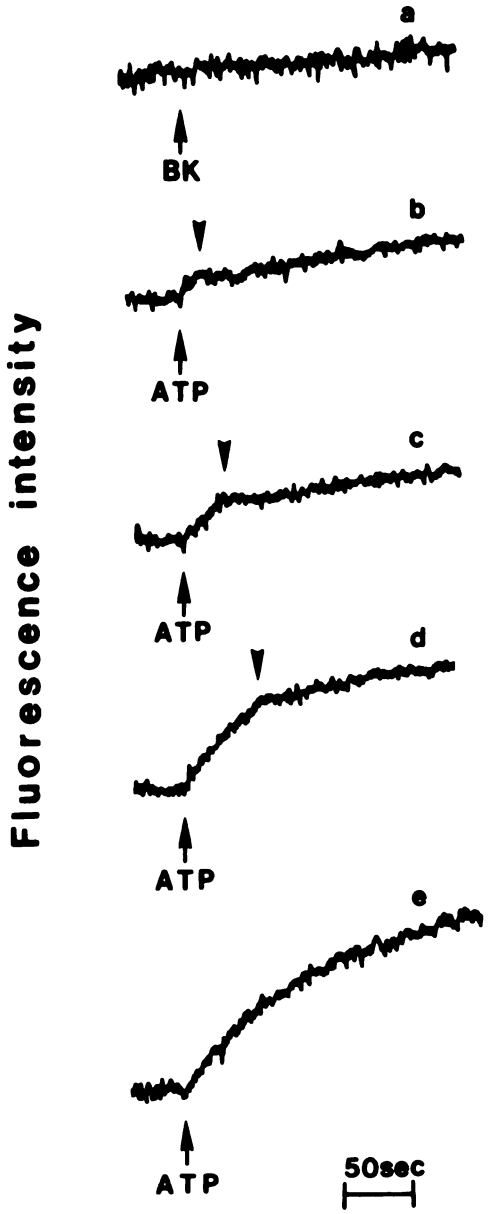

Fig. 3. Effect of Mg^{2+} on the fluorescence of DNA-ethidium bromide complexes within NG108–15 cells promoted by ATP^{4-}. ATP (3 mM) (*traces b–e*) or bradykinin (*BK*) (15 μM) (*trace a*) was added as indicated (*arrows*) to cells bathed in loading buffer containing 25 μM ethidium bromide. The entry of ethidium bromide was measured by the fluorescence of the DNA-ethidium bromide complex. Mg^{2+} (1 mM) was added to cells as indicated (*arrowheads*).

ATP was completely abolished. The IP_3 production induced by ATP was identical to that of control cells. These results are consistent with $[Ca^{2+}]_i$ measurements from our previous studies (11). In nondifferentiated cells, IP_3 generation elicited by ATP or bradykinin was slightly less than in differentiated cells (Table 1). Similarly, the responses of IP_3 generation to agonist stimulation were reduced when Ca^{2+} was removed from the extracellular buffer. Residual IP_3 generation activated by ATP still remained in the absence of extracellular Ca^{2+} in nondifferentiated cells, however.

ATP-stimulated $^{45}Ca^{2+}$ uptake within NG108–15 cells is illustrated in Fig. 4. $^{45}Ca^{2+}$ accumulation stimulated by ATP continued to increase almost linearly for >10 min, whereas the $^{45}Ca^{2+}$ uptake activated by bradykinin was negligible. Saturation of $^{45}Ca^{2+}$ accumulation was not attained until 16 min after ATP addition. The mean maximal $^{45}Ca^{2+}$ accumulation was 110.4 ± 9.3 nmol of Ca^{2+}/mg (n = 4) (Fig. 4A). Fig. 4B depicts the ATP dependence of $^{45}Ca^{2+}$ uptake in the presence or absence of Mg^{2+}. A biphasic relationship existed between ATP concentration and $^{45}Ca^{2+}$ uptake. ATP levels higher than 3 mM inhibited uptake. In the absence of exogenously added Mg^{2+}, a similar biphasic relationship between ATP concentration and $^{45}Ca^{2+}$ uptake was observed (Fig. 4B); the maximum $^{45}Ca^{2+}$ uptake was about 40% less than that in the presence of Mg^{2+}.

The effects of a variety of nucleotides and ATP analogues on $^{45}Ca^{2+}$ accumulation are demonstrated in Table 2. ADP at 3 mM caused an increase in $^{45}Ca^{2+}$ accumulation that was 29% of ATP action. However, AMP at the same concentration had no significant effect on $^{45}Ca^{2+}$ uptake (Table 2). Among the nonhydrolyzable ATP analogues, ATPγS was more potent than AMPPNP or AMPPCP in stimulation of $^{45}Ca^{2+}$ uptake (Table 2). The P_{2x} agonist AMPCPP, the P_{2y} agonist 2-MeS-ATP,

TABLE 1

Effect of extracellular Ca^{2+} on IP_3 generation stimulated by ATP or bradykinin in differentiated or nondifferentiated NG108-15 cells

Aliquots of differentiated or nondifferentiated cells (about 0.6 mg of cell protein) were stimulated with 3 mM ATP, 15 μM bradykinin, or buffer at room temperature for 15 sec, in either loading buffer or Ca^{2+}-free loading buffer. IP_3 was extracted and determined by radioreceptor assay, as described in Materials and Methods. Results are mean ± standard deviation values of triplicate experiments.

	IP_3			
	Differentiated cells		Nondifferentiated cells	
	$+Ca^{2+}$	$-Ca^{2+}$	$+Ca^{2+}$	$-Ca^{2+}$
	pmol/mg			
Basal	11.1 ± 1.3	5.6 ± 1.8	5.8 ± 0.9	2.6 ± 0.2
ATP	48.1 ± 5.1	5.8 ± 1.0	33.1 ± 1.6	5.2 ± 0.6
Bradykinin	53.8 ± 3.2	24.8 ± 5.7	38.4 ± 3.9	13.9 ± 1.4

CTP, GTP, and UTP all slightly affected $^{45}Ca^{2+}$ accumulation (Table 2).

Agents including Reactive Blue 2 (Cibacron Blue 3GA and Basilen Blue E-3G), PCMPS, and DIDS have been studied for their P_2 purinoceptor antagonist activities (22). We next examined their potency as antagonists of ATP-stimulated $^{45}Ca^{2+}$ uptake. All reagents at the indicated concentrations were individually added to the $^{45}Ca^{2+}$ uptake reaction mixture, and after 16 min at 37° the $^{45}Ca^{2+}$ accumulated within cells was measured. In the absence of antagonists, the mean maximal ATP-stimulated $^{45}Ca^{2+}$ uptake was 116.4 ± 19.3 nmol/mg (n = 29). The inhibition by antagonists was expressed as the percentage of total $^{45}Ca^{2+}$ uptake in the absence of antagonists, as shown in Figs. 5 and 6. Fig. 5 suggests that Cibacron Blue 3GA and Basilen Blue E-3G inhibited ATP-evoked $^{45}Ca^{2+}$ uptake in a concentration-dependent manner; the IC_{50} values were 3 μM and 10 μM, respectively. Similarly, DIDS antagonized ATP-induced $^{45}Ca^{2+}$ uptake, with an IC_{50} of 15 μM. A sulfhydryl reagent, PCMPS, also acted as a purinoceptor antagonist in NG108–15 cells, with an IC_{50} of 35 μM (Fig. 5).

To further characterize ATP-stimulated $^{45}Ca^{2+}$ uptake, we measured the effect of divalent cations, trivalent cations, and several compounds that have been reported to affect Ca^{2+} flux. Vanadate was ineffective up to 1 mM, and only at 1 mM did ryanodine inhibit $^{45}Ca^{2+}$ uptake (Fig. 6A). TMB-8 was ineffective up to 30 μM, but at higher concentrations it blocked ATP-induced $^{45}Ca^{2+}$ uptake significantly (Fig. 6A). Ruthenium red and diltiazem did not inhibit uptake at concentrations below 10 μM but partially inhibited $^{45}Ca^{2+}$ uptake at higher concentrations tested (Fig. 6A). Of the divalent and trivalent cations, the most effective ion for blocking ATP-stimulated $^{45}Ca^{2+}$ uptake was Cd^{2+}, with an IC_{50} of 1 μM (Fig. 6B). Nickel, cobalt, and strontium ions were uniformly much less potent than cadmium in blocking $^{45}Ca^{2+}$ uptake. Barium, manganese, and lanthanum did not affect ATP-evoked $^{45}Ca^{2+}$ uptake at concentrations up to 100 μM.

To examine the effect of P_2 purinoceptor activation on the cAMP signaling pathway, we measured cAMP production in NG108–15 cells in response to stimulation by a variety of agonists. The basal cAMP accumulation during a 15-min incubation period at 37° was 87.8 ± 0.4 pmol/mg (n = 3) (Fig. 7). Prostaglandin E_1 at 1 μM induced an increased cAMP generation of 308.3 ± 20.9 pmol/mg (n = 3), whereas leucine enkephalin at 10 μM decreased the cAMP level to 62.8 ± 9.0 pmol/mg (n = 3) (Fig. 7). ATP and bradykinin did not significantly affect the cAMP signaling pathway; the cAMP values were 91.3 ± 7.5 pmol/mg and 100.2 ± 10.4 pmol/mg upon ATP and bradykinin stimulation, respectively (Fig. 7).

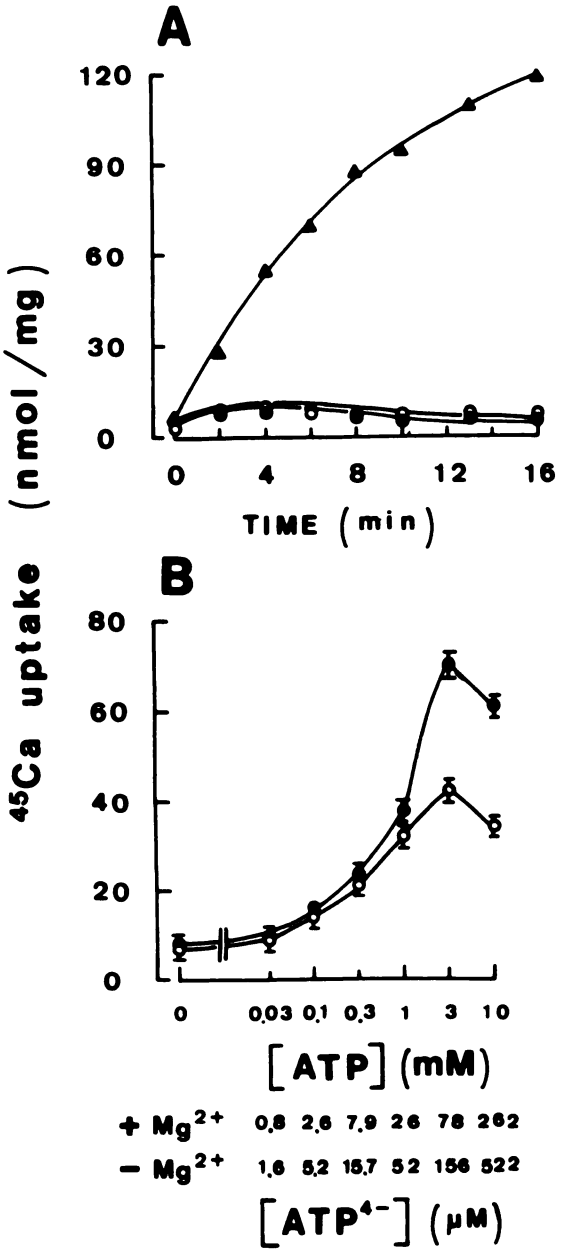

Fig. 4. Time, concentration, and Mg^{2+} dependence of $^{45}Ca^{2+}$ uptake stimulated by ATP or bradykinin in NG108–15 cells. A, The time dependence of $^{45}Ca^{2+}$ uptake is shown after addition of 3 mM ATP (▲), 15 μM bradykinin (●), or buffer (○). B, The effect of Mg^{2+} on the ATP dependence of $^{45}Ca^{2+}$ uptake is shown. $^{45}Ca^{2+}$ uptake was measured for 5 min after addition of ATP at the concentrations shown and proceeded in the presence (●) or in the absence (○) of Mg^{2+}. The concentrations of ATP^{4-} shown were calculated according to an equation described previously (29). Data described are the mean ± standard deviation of three independent experiments.

Discussion

We have identified and characterized the response pathways induced by ATP in neuroblastoma × glioma NG108–15 cells. These responses are clearly distinguishable from bradykinin-induced reactions, which are present within the same cells. Previously, we showed that ATP induces Ca^{2+} influx in NG108–15 cells (11). Two possible mechanisms for Ca^{2+} influx have been proposed; ATP may directly activate a receptor-operated cation channel that is permeable to Ca^{2+} and Na^+, or ATP^{4-} may promote pore formation in the plasma membrane, allowing

TABLE 2

Effect of nucleotides and ATP analogues on $^{45}Ca^{2+}$ uptake in NG108-15 cells

Aliquots of NG108-15 cells (0.4 mg of cell protein) were incubated with 3 mM concentrations of the indicated nucleotides in 220 μl of loading buffer containing $^{45}Ca^{2+}$. Uptake was determined at 37° for 16 min, as described in Materials and Methods. The response induced by 3 mM ATP is expressed as 100%. Data are mean ± standard deviation calculated from triplicate experiments.

Compound	$^{45}Ca^{2+}$ uptake	Response
	nmol of Ca^{2+}/mg	%
Control	9.8 ± 0.3	9
ATP	101.1 ± 1.0	100
ADP	29.3 ± 1.0	29
AMP	9.1 ± 0.3	9
ATPγS	79.7 ± 1.5	79
AMPPNP	19.2 ± 1.1	19
AMPPCP	21.2 ± 0.1	21
AMPCPP	15.1 ± 0.2	15
2-MeS-ATP	22.2 ± 1.0	22
CTP	23.2 ± 1.0	23
UTP	18.1 ± 0.2	18
GTP	19.2 ± 0.8	19

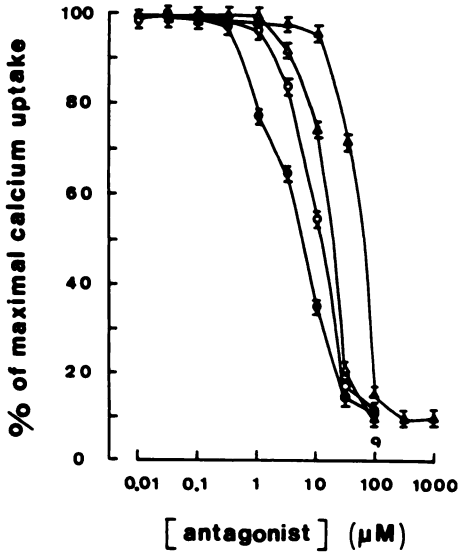

Fig. 5. Inhibition of ATP-elicited $^{45}Ca^{2+}$ uptake by purinoceptor antagonists. Basilen Blue E-3G (○), Cibacron Blue 3GA (●), DIDS (△), or PCMPS (▲) was added to the cells at the indicated concentrations, simultaneously with 3 mM ATP. $^{45}Ca^{2+}$ uptake was measured for 16 min after ATP addition. The inhibition by various antagonists is presented as a percentage of maximal $^{45}Ca^{2+}$ uptake. The mean maximal Ca^{2+} uptake in the absence of antagonists was 116.4 ± 19.3 nmol/mg (n = 29). Results shown are the mean ± standard deviation from three independent experiments.

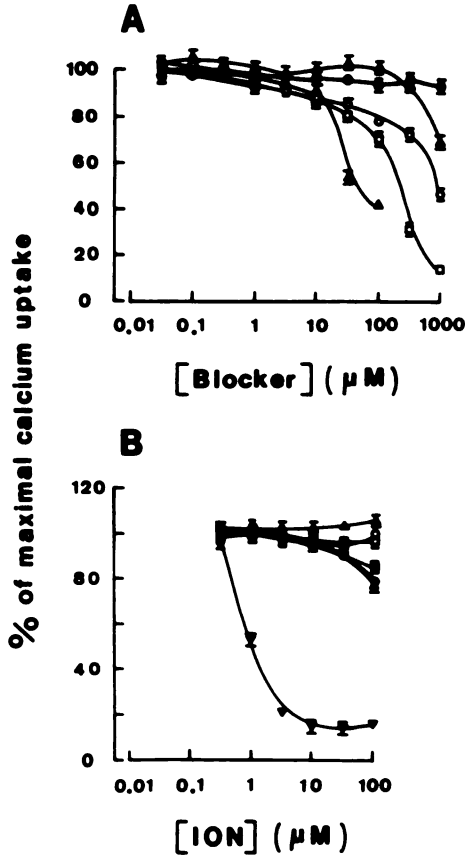

Fig. 6. Effect of various agents and cations on ATP-evoked $^{45}Ca^{2+}$ uptake in NG108–15 cells. A, Vanadate (●), ryanodine (△), diltiazem (○), TMB-8 (□), and ruthenium red (▲) at the indicated concentrations were added to cells simultaneously with 3 mM ATP. B, Divalent cations Mn^{2+} (△), Ba^{2+} (□), Sr^{2+} (■), Ni^{2+} (●), Co^{2+} (▲), and Cd^{2+} (▼), as well as the trivalent cation La^{3+} (○), at the indicated concentrations, were added to cells together with 3 mM ATP. After 16 min, $^{45}Ca^{2+}$ accumulation within cells was determined; the total amount of $^{45}Ca^{2+}$ taken up without any added agents or cations was 116.4 ± 19.3 nmol/mg (n = 29). The inhibition by various agents and cations is presented as a percentage of total $^{45}Ca^{2+}$ uptake. Data are the mean ± standard deviation from three independent experiments.

molecules smaller than 831 kDa to pass through. Here we show that in NG108–15 cells ATP induced an increase in $[Ca^{2+}]_i$ that was inversely dependent on external Na^+ (Fig. 1) and Na^+ influx was stimulated by ATP (Fig. 2). Our findings suggest that a nonselective cation channel is activated by ATP in NG108–15 cells. Indeed, ATP-stimulated $^{45}Ca^{2+}$ uptake into NG108–15 cells could be inhibited by ATP-sensitive cation channel blockers, such as DIDS, Cibacron Blue 3GA, Basilen Blue E-3G, and PCMPS (Figs. 4 and 5) (22). In addition, direct evidence demonstrates that pores formed by ATP^{4-} are also responsible for the action of ATP in NG108–15 cells. The entry of ethidium bromide induced by ATP was inhibited by Mg^{2+} (Fig. 3). Furthermore, no second messenger generation in response to ATP was observed in this study (Fig. 7; Table 1), although activation of phospholipase C or adenylate cyclase has been proposed to be coupled with occupancy of P_2 purinoceptors in other cell types (1, 8). The results described above indicate that two distinct ATP signaling mechanisms operate in NG108–15 cells.

Because NG108–15 cells possess ATP purinoceptors (11), activation of ATP-sensitive channels could plausibly induce entry of Na^+ and Ca^{2+}. Previously we have shown that (i) the effect of ATP on $[Ca^{2+}]_i$ rise is specific, inasmuch as other nucleotides are less effective; (ii) external Ca^{2+} is absolutely required for observation of the $[Ca^{2+}]_i$ rise induced by ATP; and (iii) the ATP-induced $[Ca^{2+}]_i$ change is not affected by the level of filling of internal Ca^{2+} pools (11). Here we further demonstrate that (i) $^{45}Ca^{2+}$ uptake is specifically stimulated by ATP (Fig. 4); (ii) a negative linear relationship exists between the concentration of Na^+ and changes in $[Ca^{2+}]_i$ induced by ATP (Fig. 1); (iii) Na^+ influx is induced by ATP (Fig. 2); (iv) $^{45}Ca^{2+}$ uptake stimulated by ATP can be efficiently inhibited by Cibacron Blue 3GA, Basilen Blue E-3G, DIDS, and PCMPS (Fig. 5); and (v) no change in IP_3 or cAMP generation occurs in response to ATP (Fig. 7; Table 1). We present no direct evidence that the observed Na^+ and Ca^{2+} influx is related to a

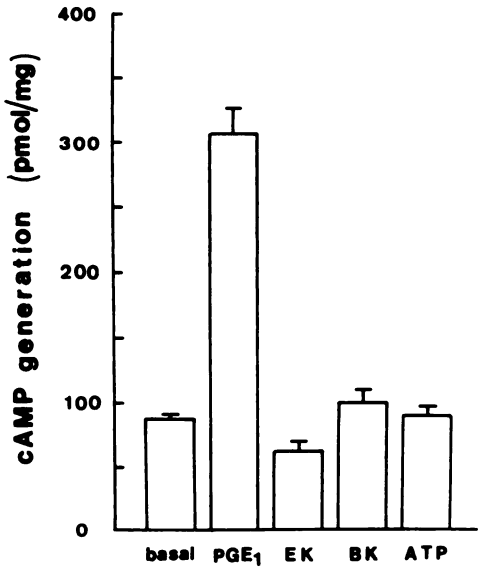

Fig. 7. Effect of various agonists on cellular cAMP accumulation. After incubation with 0.5 mM IBMX for 30 min in culture, aliquots of cells (0.6 mg of cell protein) were stimulated at 37° for 15 min with 1 μM prostaglandin E_1 (*PGE_1*), 10 μM leucine enkephalin (*EK*), 3 mM ATP, 15 μM bradykinin (*BK*), or buffer (*basal*), as indicated. Cellular cAMP accumulation was determined as described in Materials and Methods. Results are mean ± standard deviation values of triplicate experiments.

specific receptor subclass. Nevertheless, our findings are consistent with the hypothesis that ATP activates a cation channel that is nonselectively permeable to Na^+ and Ca^{2+} in various cell types, e.g., sensory neurons (23), lacrimal acinar cells (24), arterial smooth muscle cells (25), ventricular myocytes (26), urinary bladder cells (27), hepatoma cells (28), and PC12 cells (14).

We previously suggested that P_{2z} purinoceptors may be responsible for Ca^{2+} influx in NG108–15 cells (11). Recently, other investigators have shown that the magnitude of the increase in $[Ca^{2+}]_i$ elicited by ATP correlates with the concentration of ATP^{4-} in the medium and not with the concentration of $MgATP^{2-}$ in NG108–15 cells (21). Pores formed by ATP^{4-} can be detected by observing the uptake of the fluorescent dye ethidium bromide, which stains DNA (6, 18). In this study, a large increase in fluorescence was observed at an ATP^{4-} concentration of 78.5 μM and was halted by addition of excess Mg^{2+}, indicating that ATP^{4-} was the active ATP species.

If the changes in $[Ca^{2+}]_i$ were entirely dependent on the nonselective pores formed by ATP^{4-}, it seems unlikely that the $[Ca^{2+}]_i$ change would be negatively correlated with external Na^+ concentration (Fig. 1). Therefore, nonselective pores formed by ATP^{4-} are only partially responsible for the Ca^{2+} influx in NG108–15 cells. Other data also argue against ATP^{4-}-formed pores being exclusively involved. Firstly, the maximal $^{45}Ca^{2+}$ uptake evoked by ATP in the absence of Mg^{2+} was 40% less than uptake in the presence of Mg^{2+} (Fig. 4). In the presence of Mg^{2+}, the concentration of ATP required to induce half-maximal $^{45}Ca^{2+}$ uptake was greater. However, the calculated EC_{50} values of ATP^{4-} according to an equation described previously (29) for $^{45}Ca^{2+}$ uptake were close, i.e., 26.2 μM and 23.2 μM in the presence and absence of Mg^{2+}, respectively (Fig. 4). This result indicates that, in addition to ATP^{4-}, $MgATP^{2-}$ also plays a role in Ca^{2+} flux. In addition, $^{45}Ca^{2+}$ uptake in response to ATP should not be efficiently blocked by purinoceptor antagonists (Fig. 5) if $^{45}Ca^{2+}$ uptake occurs via ATP^{4-}-formed pores. In contrast to our present study, when we previously measured $[Ca^{2+}]_i$ rise evoked by ATP the action of ATP was inhibited by Mg^{2+} (11). If Mg^{2+} is required to remove increased cytosolic Ca^{2+}, a greater $[Ca^{2+}]_i$ rise would be expected in the absence of Mg^{2+} due to the slower action, which might account for the difference in results.

The enhancement of $^{45}Ca^{2+}$ uptake by Mg^{2+} indicates that $MgATP^{2-}$ actively induces plasma membrane Ca^{2+}-permeable channels. The ineffectiveness of nonhydrolyzable ATP analogues in $^{45}Ca^{2+}$ uptake (Table 2) and in $[Ca^{2+}]_i$ rise (11) implies that an ATPase or a kinase is involved in ATP action in NG108–15 cells. $MgATP^{2-}$ is required for either ATPase or kinase action. Indeed, NG108–15 cells display ectokinase activity (30), and ATP-induced $^{45}Ca^{2+}$ uptake correlates with surface protein phosphorylation activity (31). Consistent with our hypothesis, in ventricular myocytes an ATP-mediated phosphorylation mechanism has recently been proposed to be responsible for the ATP-stimulated Ca^{2+} influx (26). At present we have no explanation for the stimulation of $^{45}Ca^{2+}$ uptake by ATPγS (Table 2).

We have recently shown that bradykinin and ATP activate distinct signaling mechanisms (11); the ATP-stimulated $[Ca^{2+}]_i$ rise was dependent on external Ca^{2+} and was insensitive to thapsigargin, whereas the bradykinin-stimulated rise was independent of external Ca^{2+} and was sensitive to thapsigargin. This suggests that bradykinin triggers internal Ca^{2+} release via IP_3 generation, whereas ATP activates a Ca^{2+}-permeable channel. Similar observations have been reported for PC12 pheochromocytoma cells (14). Evidence from our present study supports previous findings. Firstly, activation of IP_3 generation by ATP was completely inhibited by removal of external Ca^{2+} in dibutyryl-cAMP-treated cells, whereas bradykinin-mediated IP_3 generation remained unaltered (Table 1). Secondly, Na^+ influx, entry of ethidium bromide, or $^{45}Ca^{2+}$ uptake, activated by ATP, did not respond to bradykinin (Figs. 2–4). Our results show that ATP and bradykinin regulate Ca^{2+} homeostasis in dibutyryl-cAMP-differentiated NG108–15 cells by very different mechanisms.

In contrast to our findings, ATP has been reported to induce an increase in $[Ca^{2+}]_i$ in the absence of external Ca^{2+} in NG108–15 cells (21, 32). In addition, UTP also induces $[Ca^{2+}]_i$ rise in NG108–15 cells (21). However, in agreement with our findings, other investigators have demonstrated that the ATP-mediated $[Ca^{2+}]_i$ rise is blocked by the removal of extracellular Ca^{2+} and ATP-induced $[^3H]IP$ accumulation is largely inhibited in the presence of La^{3+} to block Ca^{2+} entry in NG108–15 cells (31). Unlike the cells in our study, the cells used in those studies had not been treated with dibutyryl-cAMP, which might explain the difference in results. When we used untreated NG108–15 cells (nondifferentiated cells), the IP_3 generation activated by ATP was still observed in the absence of external Ca^{2+} (Table 1). Recently, it has been shown that removal of extracellular Ca^{2+} reduces but does not block opioid-induced $[Ca^{2+}]_i$ rise in nondifferentiated NG108–15 cells, whereas the response is completely blocked by removal of extracellular Ca^{2+} in differentiated cells (33). In the presence of extracellular Ca^{2+}, IP_3 generation in response to ATP might be due to the indirect activation of phospholipase C by the influx of Ca^{2+} stimulated by ATP (Table 1) (34).

In general, P_2 purinoceptor subclassification is entirely based on the potencies of the responses to various agonists (2). Using dibutyryl-cAMP-differentiated NG108–15 cells, we previously

demonstrated that the P_{2x} agonist AMPCPP, the P_{2y} agonist 2-MeS-ATP, and UTP each had no effect on the $[Ca^{2+}]_i$ change (11). In this study, the nucleotides AMPCPP, 2-MeS-ATP, and UTP showed little ability to activate $^{45}Ca^{2+}$ uptake in the same cells, i.e., approximately 2 times basal activity, as opposed to 10-fold activity for ATP (Table 2). On the basis of our observations, P_{2x}, P_{2y}, and P_{2u} receptor subclasses are not involved in the Ca^{2+} flux mechanism in differentiated NG108–15 cells; P_{2z} receptors are very likely partially responsible.

Inorganic Ca^{2+} channel blockers such as Cd^{2+}, Ni^{2+}, and Gd^{3+} have been used to distinguish the subclass of voltage-sensitive Ca^{2+} channels in differentiated NG108–15 cells (35). Cd^{2+} but not other ions significantly inhibited the ATP-stimulated $^{45}Ca^{2+}$ uptake (IC_{50} = 1 μM) (Fig. 6), which suggests that the ATP channel acts as a voltage-sensitive Ca^{2+} channel. In our study ATP stimulated Na^+ influx (Fig. 2), which may have activated the voltage-sensitive Ca^{2+} channels. However, the ATP channel itself is not a voltage-sensitive Ca^{2+} channel, because a larger ATP response was observed in Na^+-free solution (Fig. 1). On the other hand, the supersensitivity of ATP action to Cd^{2+} in NG108–15 cells differs from the situation in PC12 cells, where Cd^{2+} at up to 300 μM is ineffective in inhibiting ATP-mediated secretion (36, 37).

In conclusion, our evidence suggests that ATP responses in dibutyryl-cAMP-treated NG108–15 cells are mediated by two distinct pathways, i.e., pores formed by ATP^{4-} and a cation channel permeable to Na^+ and Ca^{2+}.

References

1. El-Moatassim, C., J. Dornand, and J.-C. Mani. Extracellular ATP and cell signalling. *Biochim. Biophys. Acta* **1134**:31–45 (1992).
2. O'Connor, S. E., I. A. Dainty, and P. Leff. Further subclassification of ATP receptors based on agonist studies. *Trends Pharmacol. Sci.* **12**:137–141 (1991).
3. Wilkinson, G. F., J. R. Purkiss, and M. R. Boarder. The regulation of aortic endothelial cells by purines and pyrimidines involves co-existing P_{2y}-purinoceptors and nucleotide receptors linked to phospholipase C. *Br. J. Pharmacol.* **108**:689–693 (1993).
4. Bean, B. P. Pharmacology and electrophysiology of ATP-activated ion channels. *Trends Pharmacol. Sci.* **13**:87–90 (1992).
5. Illes, P., and W. Norenberg. Neuronal ATP receptors and their mechanism of action. *Trends Pharmacol. Sci.* **14**:50–54 (1993).
6. Tatham, P. E. R., and M. Lindau. ATP-induced pore formation in the plasma membrane of rat peritoneal mast cells. *J. Gen. Physiol.* **95**:459–476 (1990).
7. El-Moatassim, C., J.-C. Mani, and J. Dornand. Extracellular ATP^{4-} permeabilizes thymocytes not only to cations but also to low-molecular-weight solutes. *Eur. J. Pharmacol.* **181**:111–118 (1990).
8. Sato, K., F. Okajima, and Y. Kondo. Extracellular ATP stimulates three different receptor-signal transduction systems in FRTL-5 thyroid cells. *Biochem. J.* **283**:281–287 (1992).
9. Lustig, K. D., L. Erb, M. G. Sportiello, D. M. Landis, C. S. Hicks-Taylor, X. Zhang, and G. A. Weisman. Mechanisms by which extracellular ATP and UTP stimulate the release of prostacyclin from bovine pulmonary artery endothelial cells. *Biochim. Biophys. Acta* **1134**:61–72 (1992).
10. Martin, T. W., and K. Michaelis. P_2-purinergic agonists stimulate phosphodiesteratic cleavage of phosphatidylcholine in endothelial cells. *J. Biol. Chem.* **264**:8847–8856 (1989).
11. Chueh, S. H., and L. S. Kao. Extracellular ATP stimulates calcium influx in neuroblastoma × glioma hybrid NG108–15 cells. *J. Neurochem.* **61**:1782–1788 (1993).
12. Yano, K., H. Higashida, R. Inoue, and Y. Nozawa. Bradykinin-induced rapid breakdown of phosphatidylinositol 4,5-bisphosphate in neuroblastoma × glioma hybrid NG108–15 cells. *J. Biol. Chem.* **259**:10201–10207 (1984).
13. Berridge, M. J. Inositol trisphosphate and calcium signalling. *Nature (Lond.)* **361**:315–325 (1993).
14. Reber, B. F. X., R. Neuhaus, and H. Reuter. Activation of different pathways for calcium elevation by bradykinin and ATP in rat pheochromocytoma (PC12) cells. *Pfluegers Arch.* **420**:213–218 (1992).
15. McMillian, M. K., S. P. Soltoff, L. C. Cantley, R. Rudel, and B. R. Talamo. Two distinct cytosolic calcium responses to extracellular ATP in rat parotid acinar cells. *Br. J. Pharmacol.* **108**:453–461 (1993).
16. Grynkiewicz, G., M. Poenie, and R. Y. Tsien. A new generation of Ca^{2+} indicators with greatly improved fluorescence properties. *J. Biol. Chem.* **260**:3440–3450 (1985).
17. Harootunian, A. T., J. P. Y. Kao, B. K. Eckert, and R. Y. Tsien. Fluorescence ratio imaging of cytosolic free Na^+ in individual fibroblasts and lymphocytes. *J. Biol. Chem.* **264**:19458–19467 (1989).
18. Tatham, P. E. R., N. J. Cusack, and B. D. Gomperts. Characterisation of the ATP^{4-} receptor that mediates permeabilisation of rat mast cells. *Eur. J. Pharmacol.* **147**:13–21 (1988).
19. Lowry, O. H., N. J. Rosebrough, A. L. Farr, and R. J. Randall. Protein measurement with the Folin phenol reagent. *J. Biol. Chem.* **193**:265–275 (1951).
20. Satoh, H., H. Hayashi, N. Noda, H. Terada, A. Kobayashi, Y. Yamashita, T. Kawai, M. Hirano, and N. Yamazaki. Quantification of intracellular free sodium ions by using a new fluorescent indicator, sodium-binding benzofuran isophthalate, in guinea pig myocytes. *Biochem. Biophys. Res. Commun.* **175**:611–616 (1991).
21. Lin, T.-A., K. D. Lustig, M. G. Sportiello, G. A. Weisman, and G. Y. Sun. Signal transduction pathways coupled to a P_{2u} receptor in neuroblastoma × glioma (NG108–15) cells. *J. Neurochem.* **60**:1115–1125 (1993).
22. Feden, J. S., and S. J. Lamport. P_2-purinoceptor antagonists. *Ann. N. Y. Acad. Sci.* **603**:182–197 (1990).
23. Bean, B. P. ATP-activated channels in rat and bullfrog sensory neurons: concentration dependence and kinetics. *J. Neurosci.* **10**:1–10 (1990).
24. Sasaki, T., and D. V. Gallacher. Extracellular ATP activates receptor-operated cation channels in mouse lacrimal acinar cells to promote calcium influx in the absence of phosphoinositide metabolism. *FEBS Lett.* **264**:130–134 (1990).
25. Benham, C. D., and R. W. Tsien. A novel receptor-operated Ca^{2+}-permeable channel activated by ATP in smooth muscle. *Nature (Lond.)* **328**:275–278 (1987).
26. Christie, A., V. K. Sharma, and S.-S. Sheu. Mechanism of extracellular ATP-induced increase of cytosolic Ca^{2+} concentration in isolated rat ventricular myocytes. *J. Physiol. (Lond.)* **445**:369–388 (1992).
27. Inoue, R., and A. F. Brading. The properties of the ATP-induced depolarization and current in single cells isolated from the guinea-pig urinary bladder. *Br. J. Pharmacol.* **100**:619–625 (1990).
28. Bear, C. E., and C. Li. Calcium-permeable channels in rat hepatoma cells are activated by extracellular nucleotides. *Am. J. Physiol.* **261**:C1018–C1024 (1991).
29. Cockcroft, S., and B. D. Gomperts. Activation and inhibition of calcium-dependent histamine secretion by ATP ions applied to rat mast cells. *J. Physiol. (Lond.)* **296**:229–243 (1979).
30. Ehrlich, Y. H., T. Davis, E. Bock, E. Kornecki, and R. H. Lenox. Ecto protein kinase activity on the external surface of intact neural cells. *Nature (Lond.)* **320**:67–69 (1986).
31. Ehrlich, Y. H., R. M. Snider, E. Kornecki, M. G. Garfield, and R. H. Lenox. Modulation of neuronal signal transduction systems by extracellular ATP. *J. Neurochem.* **50**:295–301 (1988).
32. Hirano, Y., F. Okajima, H. Tomura, M. A. Majid, T. Takeuchi, and Y. Kondo. Change of intracellular calcium of neural cells induced by extracellular ATP. *FEBS Lett.* **284**:235–237 (1991).
33. Jin, W., N. M. Lee, H. H. Loh, and S. A. Thayer. Dual excitatory and inhibitory effects of opioids on intracellular calcium in neuroblastoma × glioma hybrid NG108–15 cells. *Mol. Pharmacol.* **42**:1083–1089 (1992).
34. Eberhard, D. A., and W. H. Holz. Intracellular Ca^{2+} activates phospholipase C. *Trends Neurosci.* **11**:517–520 (1988).
35. Brown, D. A., R. J. Docherty, and I. McFadzean. Calcium channels in vertebrate neurons: experiments on a neuroblastoma hybrid model. *Ann. N. Y. Acad. Sci.* **560**:358–372 (1989).
36. Inoue, K., K. Nakazawa, K. Fujimori, and A. Takanaka. Extracellular adenosine 5′-triphosphate-evoked norepinephrine secretion not relating to voltage-gated Ca channels in pheochromocytoma PC12 cells. *Neurosci. Lett.* **106**:294–299 (1989).
37. Sela, D., E. Ram, and D. Atlas. ATP receptor: a putative receptor-operated channel in PC12 cells. *J. Biol. Chem.* **266**:17990–17994 (1991).

Send reprint requests to: Sheau-Huei Chueh, Department of Biochemistry, National Defense Medical Center, P.O. Box 90048–501, Taipei, Taiwan, R.O.C.